SMC-TR-95-43

AEROSPACE REPORT NO.
TR-94(4935)-5

# Ultrahigh-Vacuum High-Resolution Transmission Electron Microscopy of Sputter-Deposited $MoS_2$ Thin Films



1 September 1995

Prepared by

G. JAYARAM, N. DORAISWAMY, and L. D. MARKS
Northwestern University, Evanston, IL

M. R. HILTON
The Aerospace Corporation, El Segundo, CA

Prepared for

SPACE AND MISSILE SYSTEMS CENTER
AIR FORCE MATERIEL COMMAND
2430 E. El Segundo Boulevard
Los Angeles Air Force Base, CA 90245



Engineering and Technology Group

THE AEROSPACE CORPORATION
El Segundo, California

This report was submitted by The Aerospace Corporation, El Segundo, CA 90245-4691, under Contract No. F04701-93-C-0094 with the Space and Missile Systems Center, 2430 E. El Segundo Blvd., Los Angeles Air Force Base, CA 90245. It was reviewed and approved for The Aerospace Corporation by S. Feuerstein, Principal Director, Mechanics and Materials Technology Center.

This report has been reviewed by the Public Affairs Office (PAS) and is releasable to the National Technical Information Service (NTIS). At NTIS, it will be available to the general public, including foreign nationals.

This technical report has been reviewed and is approved for publication. Publication of this report does not constitute Air Force approval of the report's findings or conclusions. It is published only for the exchange and stimulation of ideas.

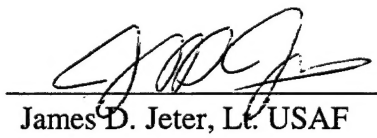

James D. Jeter, Lt. USAF
SMC/CI

# REPORT DOCUMENTATION PAGE

*Form Approved*
*OMB No. 0704-0188*



| 1. AGENCY USE ONLY (*Leave blank*) | 2. REPORT DATE | 3. REPORT TYPE AND DATES COVERED |
|---|---|---|
| | 1 September 1995 | |

4. TITLE AND SUBTITLE
Ultrahigh-Vacuum High-Resolution Transmission Electron Microscopy of Sputter-Deposited MoS2 Thin Films

5. FUNDING NUMBERS
F04701-93-C-0094

6. AUTHOR(S)
G. Jayaram, N. Doraiswamy, L. D. Marks, and M. R. Hilton

7. PERFORMING ORGANIZATION NAME(S) AND ADDRESS(ES)
The Aerospace Corporation
Technology Operations
El Segundo, CA 90245-4691

8. PERFORMING ORGANIZATION REPORT NUMBER
TR-94(4935)-5

9. SPONSORING/MONITORING AGENCY NAME(S) AND ADDRESS(ES)
Space and Missile Systems Center
Air Force Materiel Command
2430 E. El Segundo Boulevard
Los Angeles Air Force Base, CA 90245

10. SPONSORING/MONITORING AGENCY REPORT NUMBER
SMC-TR-95-43

11. SUPPLEMENTARY NOTES

12a. DISTRIBUTION/AVAILABILITY STATEMENT
Approved for public release; distribution unlimited

12b. DISTRIBUTION CODE

13. ABSTRACT (*Maximum 200 words*)

High-resolution electron microscopy has been used to characterize the structure of sputter-deposited $MoS_2$ coatings under both conventional and ultrahigh-vacuum (UHV) conditions. As deposited, the films have a mixture of short-range ordered basal-plane and edge-plane oriented grains near the film substrate interface; structural changes were characterized in a UHV transmission electron microscope as a function of two processing variables: temperature and Au deposition. Annealing in an oxygen environment was also carried out to assess chemical stability. During thermal annealing in UHV and in oxygen, substantial long-range ordering of the basal islands followed by grain growth was observed. Inhomogeneous oxidation resulting in the formation of $MoO_3$ in the initial stages followed by grain growth, yielding the final morphology of a mixture of $MoO_3$ crystallites of 5–50 nm size was seen on annealing in an oxidizing atmosphere. Au nucleation and growth on both thermally annealed and as-deposited films were seen to follow the Volmer-Weber mode. i.e., three-dimensional islands; these islands were also seen to be highly textured. Also, in comparison with carbon and SiO substrates, Au demonstrated higher stability to electron beam fluxes on $MoS_2$, suggesting higher bonding strengths to the substrate. These experiments demonstrated the paramount need for UHV conditions during both deposition and characterization to avoid uncertain contamination artifacts.

| 14. SUBJECT TERMS | 15. NUMBER OF PAGES |
|---|---|
| Solid lubricants, $MoS_2$, Bearings, Storage degradation, Oxidation | 7 |
| | 16. PRICE CODE |

| 17. SECURITY CLASSIFICATION OF REPORT | 18. SECURITY CLASSIFICATION OF THIS PAGE | 19. SECURITY CLASSIFICATION OF ABSTRACT | 20. LIMITATION OF ABSTRACT |
|---|---|---|---|
| UNCLASSIFIED | UNCLASSIFIED | UNCLASSIFIED | |

## Preface

Work was sponsored by the Air Force Materiel Command, Space and Missile Systems Center, under Contract F04701-93-C-0094 as part of The Aerospace Corporation Mission-Oriented Investigation and Experimentation Program and the US Air Force Office of Scientific Research on Grant F49620-93-1-0208 AFOSR. The authors wish to thank Reinhold Bauer (The Aerospace Corporation) for preparing the $MoS_2$ films and R. Plass and R. Passeri (Northwestern University) for designing the heater stage and preparing the SiO grids.

## Contents

## Figures

## 1. Introduction

The need for long-endurance thin solid lubricant films for precision mechanisms in spacecraft led to the development of sputter-deposited $MoS_2$ [1]. The first generation of these films had a microstructure that resulted from competitive nucleation and growth between basal-plane (i.e. the (001) planes) and edge-plane oriented grains (i.e. the (100) and the (110) planes) [2,3]. In general, pure sputter-deposited $MoS_2$ films have a porous columnar-plate morphology with an edge-plane preferred orientation parallel to the substrate surface. However, the columnar plates are in the wrong orientation for lubrication and tend to detach near the film–substrate interface and reorient into lubricating particles early in operation [1,4,5]. In addition, the edge-plane orientation also enhances the formation of $MoO_3$ when $MoS_2$ is stored (or, worse, operated) in humid air [6–8]. This oxide has significantly lesser endurance and a higher friction coefficient than $MoS_2$ [9–11]. Experiments have shown that basal-plane orientation and large grain size partially inhibit $MoO_3$ formation in humid environments [6–11].

The need to minimize early debris generation in rolling-contact applications led to the development of a second generation of sputter-deposited $MoS_2$ [12]. These films generally have denser morphologies and more basal-plane orientation because the growth of edge facets is slowed or suppressed; this is accomplished by incorporating dopants (Au, Ni, $SbO_x$, or polytetrafluoroethylene) as co-sputtered species or as multilayers [13–16]. Adjusting deposition conditions, i.e. high power densities, low pressures, and use of ion beams or lasers, also promotes a denser microstructure [17–20].

Detailed investigations of the nanostructure of these materials are incomplete. In particular, the morphological distribution of metal dopants in the newer co-sputtered and multilayer films has not been well characterized and the relationship of these nanostructures to tribological performance and humid storage stability is not well understood. There are also many issues concerning the role of contaminants in both types of film; most sputter-deposited films prepared in high vacuum systems contain 5–15 at.% oxygen (and/or carbon). Some recent results [21,22] have highlighted this very dramatically; very pure thin films of $MoS_2$ grown under ultrahigh vacuum (UHV) conditions have been found to yield friction coefficients about an order of magnitude smaller than those obtained with conventional high vacuum films.

The availability of an UHV transmission electron microscope with a modular vacuum system design that allows interconnection to deposition chambers and other analytical systems offers exciting possibilities for studies of film growth processes of many material systems. In this paper we report the first UHV transmission electron microscopy (TEM) study of sputter-deposited $MoS_2$. The aim of the present study was twofold: (1) to investi-

gate the structural and chemical stability of $MoS_2$ during thermal treatments in UHV and oxidizing environments as a function of microstructure to gain insight into storage and contamination issues; (2) to assess the desirability of connecting an $MoS_2$ deposition system to the UHV transmission electron microscope.

The UHV transmission electron microscope was used to characterize structural changes in $MoS_2$ films (which for these experiments were prepared ex situ) as a function of two deposition variables: temperature and Au deposition (executed in situ), the latter providing a basis towards understanding the structure of Au used in co-sputtering and multilayer applications.

## 2. Experimental procedures

Thin films (10–20 nm) of $MoS_2$ were deposited, by r.f. sputtering according to procedures described earlier [4] on substrates of amorphous evaporated carbon and SiO on Cu grids; the latter were used for oxygen annealing experiments. Films were prepared at substrate temperatures of 70 °C (designated AT for ambient temperature) and 220 °C (designated HT for high temperature).

Imaging was carried out in a Hitachi UHV-H9000 microscope operated at 300 keV. Thermal annealing in UHV and subsequent deposition of Au on annealed AT and HT films were carried out inside the UHV transmission electron microscope column itself. Au deposition on as-deposited AT films and heat treatment under an oxidizing atmosphere were executed in an attached chamber (sample transfer was conducted under UHV conditions). The static operating pressure inside both chambers was approximately $1 \times 10^{-8}$ Pa (for a review of the instrument, see [23]).

## 3. Results

### *3.1. As-deposited films*

Prior to any heat treatment, a microstructural map of the as-deposited thin film was obtained using UHV high resolution electron microscopy (HREM). The as-deposited film microstructure for both AT and HT films, on both carbon and SiO substrates, was dominated by basal islands. The hexagonal pattern of these basal islands can be clearly seen in Fig. 1 which shows a typical HREM image of an AT film together with an inset diffraction pattern taken from the same region. However, these domains were extremely short range ordered; in comparison, basal islands in HT films had relatively longer-range order, as shown by the arrowed regions in Fig. 2. The edge island morphology was also seen in small areas of the film; their small percentage was corroborated by low intensity rings in the diffraction patterns (DPs); thicker films had more edge islands. These edge islands were not straight, i.e. they had an associated curvature. Diffraction and image data collated from different samples indicated that the planar spacings deviated from ideal single-crystal values in certain cases.

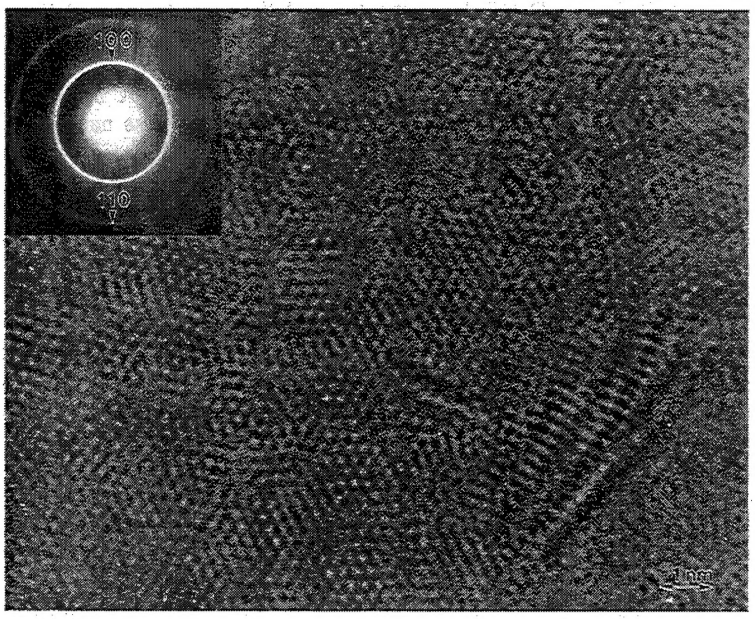


Fig. 1. The typical microstructure of an as-sputtered AT $MoS_2$ thin film, i.e. the short-range-ordered hexagonal pattern of the basal islands shown in an HREM image, together with the inset diffraction pattern showing the corresponding (100) and (110) planar spacing rings.

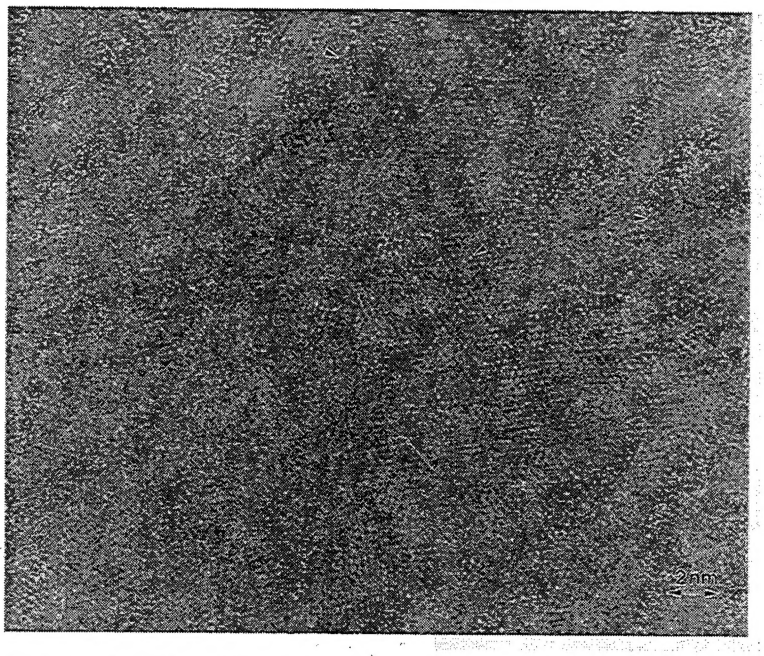


Fig. 2. A typical high resolution electron micrograph of an as-sputtered HT $MoS_2$ thin film; basal islands with relatively longer-range order (cf. Fig. 1) are arrowed.

A contraction in the spacing of the basal island fringes and an increase in the spacings of the edge island fringes were observed in these instances; these deviations are attributed to the formation of $MoS_{2-x}O_x$ which arises from oxygen, during the sample deposition, occupying substitutional sites in the $MoS_2$ lattice [24] (these structural results are consistent with earlier TEM studies of similar films by other investigators [1,25]; see also [3] for reference on earlier TEM studies of $MoS_2$.

*3.2. Thermal treatment in an ultrahigh vacuum environment*

The AT and HT films were subjected to heating cycles in the 100–550 °C range (and held at each temperature for about 10 min) in increments of roughly 50 °C. Up to 400 °C, there were no changes in film morphology in either the images or the DPs. At temperatures just above 400 °C, nucleation of small crystallites was seen in the HREM images of AT films. At 550 °C, new spotty polycrystalline rings appeared in the DPs; the corresponding HREM images showed particles with (103)- and (105)-type fringes as seen in Fig. 3. The (100) and (110) fringes still existed in the background (particles showing these fringes were also seen) with a smaller fraction of edge islands, suggesting that the film morphology consisted of a mixture of random polycrystals that had undergone a loss of texture due to heating. The intensity of the rings in the DPs suggested that particles showing (103) fringes far exceeded those showing the (105) type.

In contrast with AT films, HT films showed greater stability to such heat treatments. The HT films when heated to 550 °C showed only the initial nucleation of very small domains, arrowed in Fig. 4 (similar to the behavior of AT films on heating to 400 °C), suggesting that further heat treatment was required before domains of the size seen in the AT films heated to 550 °C could be observed. The small size of the domains in the HT film could also be inferred from the DPs where no new polycrystalline rings could be seen.

*3.3. Thermal treatment in an oxygen atmosphere*

When the AT film was further annealed at 550 °C for 5 min in a partial pressure of oxygen of approximately $1 \times 10^{-5}$ Pa, no change in morphology was observed, i.e. particles showing (103) and (105) fringes still existed in the images. However, after an anneal at the same temperature for 10 min in a partial pressure of oxygen of $1 \times 10^{-4}$ Pa, a few new particles were evident coexisting with $MoS_2$. HREM images of these particles enabled their positive identification as $MoO_3$; inhomogeneous oxidation had occurred and the absence of any ring in the DPs corresponding to the oxide indicated a small population.

The identification of $MoO_3$ was further confirmed during a 2 h time sequence under the electron beam which showed that these particles underwent radiation damage ($MoO_3$ as the maximum valent transition metal oxide undergoes radiation damage while $MoO_2$ does not [26]). Fig. 5 shows the early stages of this process for such an oxide particle; as the particle amorphized, it

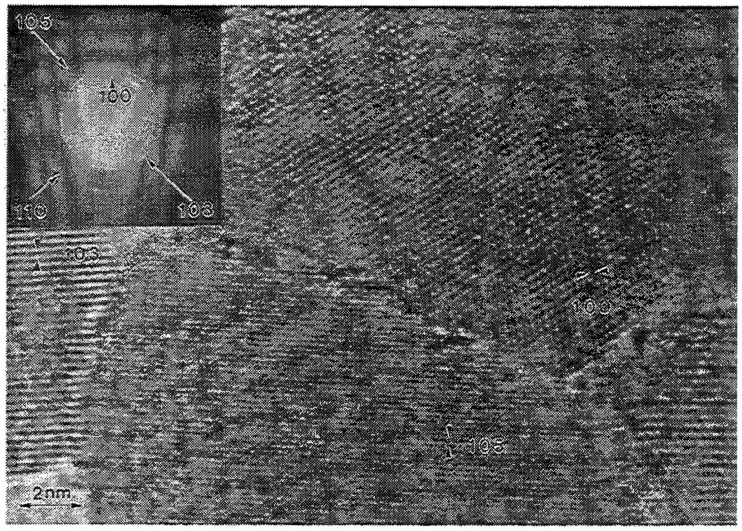


Fig. 3. Particles which show the (103) and (105) fringes and which dominate the morphology of an AT film annealed to 500–550 °C in an UHV environment. The relative intensities of the corresponding rings in the inset diffraction pattern are proportional to their population density.

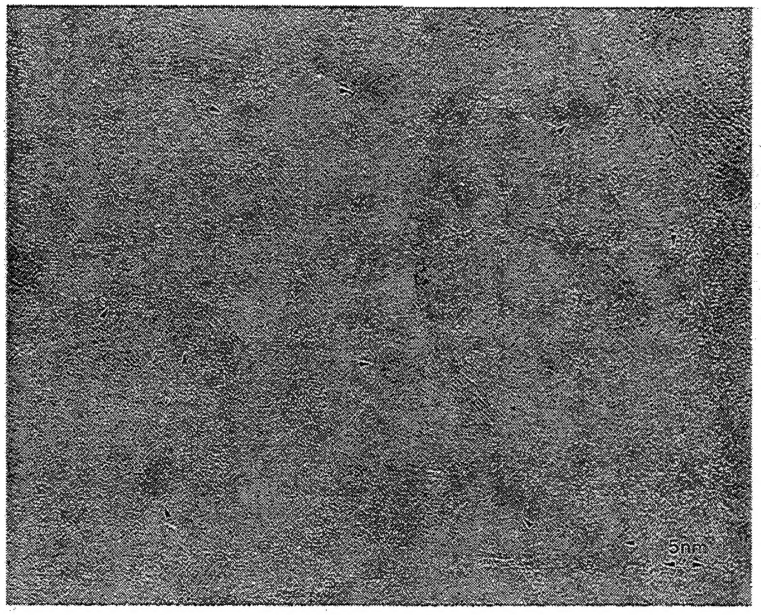


Fig. 4. The microstructure of an HT film annealed to 500–550 °C in an UHV environment identical with that in Fig. 2 with one very subtle change, i.e. the arrowed darker contrast regions which represent nucleation of very small domains similar to those seen in AT films annealed to 400 °C.

reduced to Mo metal which later crystallized under the electron beam. Electron beam exposure during this time period also caused the edge islands of $MoS_2$ to amorphize; however, the basal islands still remained crystalline during the same period of observation.

As the film was heated to higher temperatures, i.e. between 700 and 800 °C under an oxygen partial pressure of $1 \times 10^{-4}$ Pa, significant coarsening of the film occurred, resulting in particles of sizes ranging from 5 to 50 nm as seen in Fig. 6. While the image provides no information on the particles' orientation or chemistry, the inset DP revealed gross changes in the latter. Rings corresponding to the basal islands had disappeared; instead, spotty rings corresponding to the (300), (310), (410) and (420) spacings of $MoO_3$ were seen, i.e. the film had undergone complete oxidation.

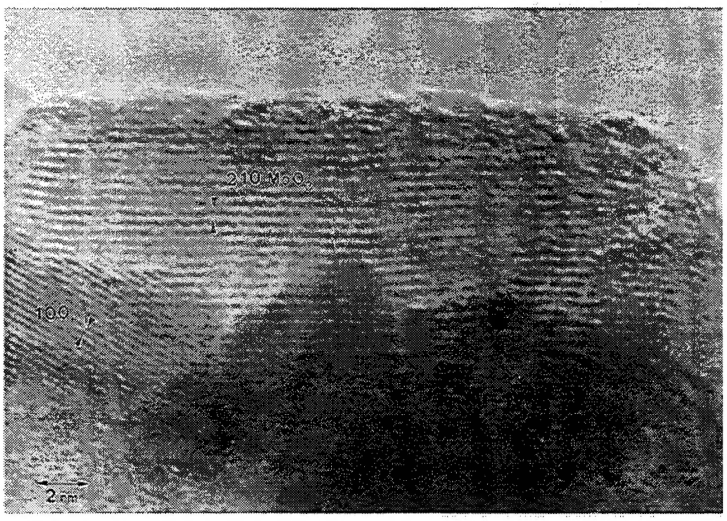


Fig. 5. Inhomogeneous oxidation which results in $MoO_3$ particles and which occurs on AT films annealed to 500–550 °C in $O_2$ at $1 \times 10^{-4}$ Pa. The amorphized fringes at the edges of the particle demonstrate the early stages of radiation damage.

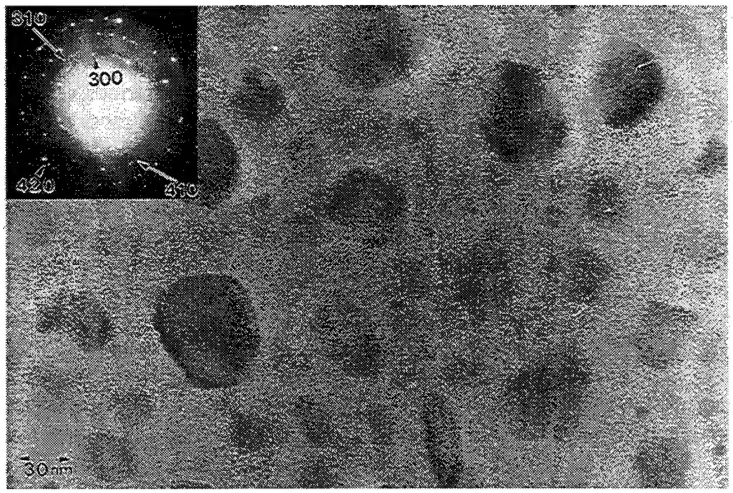


Fig. 6. Film coarsening which yields 5–50 nm particles of $MoO_3$ and which occurs on annealing AT films to 700–800 °C in $O_2$ at $1 \times 10^{-4}$ Pa. Spotty polycrystalline rings in the inset diffraction pattern reveal their orientation; the absence of the $MoS_2$ rings suggests complete oxidation.

### *3.4. Au deposition on $MoS_2$ films*

Au in the submonolayer to a few(4–5)-monolayer (ML) regime was deposited onto both as-deposited AT films and post-annealed AT and HT films. Irrespective of the thickness regime, Au growth was in the form of three-dimensional (3D) islands on all types of film (at higher thicknesses, Au islands simply grew in size). Fig. 7 is an HREM image of the very early stages of growth of Au ($\leqslant 1$ ML or less) on an as-deposited AT film with the inset DP showing the (111) ring of Au. On further deposition (up to 2 ML), only an increase in the intensity of the (111) ring of Au was observed. The (200) and (220) rings of Au began to appear on subsequent deposition; these were, however, very weak in intensity in comparison with the (111) ring, suggesting that Au growth on $MoS_2$ was highly textured. The HREM images also demonstrated that there seemed to be no preferential site, i.e. basal or edge, for the nucleation and growth of Au on either the AT or the HT films.

A very surprising result was that in comparison with other substrates, e.g. carbon or SiO, Au had a much higher stability when deposited on $MoS_2$. Even with high beam flux values, i.e. two orders of magnitude higher than those used in earlier studies of Au on carbon

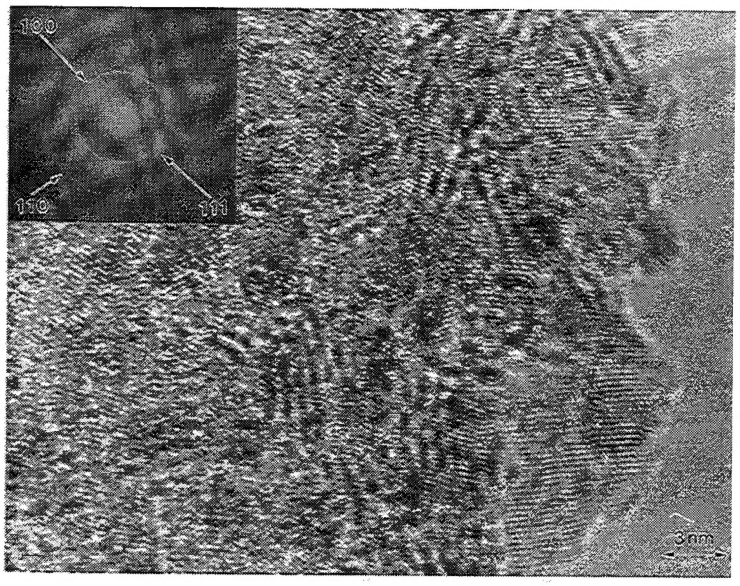


Fig. 7. Early stage of Au nucleation and growth on an as-deposited AT film; the growth mode is Volmer–Weber. The (111) ring in the inset diffraction pattern reveals the highly textured nature of this process.

or Au on SiO [27], Au particles on $MoS_2$ did not fluctuate under the beam, suggesting a very strong particle–substrate interaction.

## 4. Discussion

From the characterization data of films as deposited and after thermal annealing in UHV and in oxygen, a consistent description of these films emerges. The sputter-deposited films are nanophase materials which, near the substrate, consist primarily of basal oriented regions with edge oriented islands dispersed throughout. The basal oriented regions have nanometer-scale grains, subgrains or domains. In a thermodynamic sense, these films are more defective or are farther from a single-crystal reference material than $MoS_2$ crystals or particles used in bonded lubricants. Hence one would expect the deposited films to be metastable relative to molybdenite crystals. Such (albeit small) molybdenite crystals are used in some bonded lubricant films. In applications where the designer has a choice of using either sputter-deposited or bonded $MoS_2$, the sputter-deposited films will have less oxidation resistance in humid storage owing to the nanocrystalline structure of the $MoS_2$ and the lack of protective encapsulation that some binders provide [28].

Upon heating in vacuum, recrystallization occurs as evidenced by the 3D particles with (103) and (105) fringes. The data show that the AT films are less stable than the HT films; this is consistent with the shorter-range order of the AT films. In the time periods studied (less than 15 min) at 550 °C, an oxygen atmosphere at $1 \times 10^{-4}$ Pa ($10^{-6}$ Torr) was required to cause $MoO_3$ to form. This agrees well with other oxidation studies which report slightly lower temperatures albeit with higher oxygen pressures, e.g. in an in-situ TEM study of $MoS_2$ flakes, Baker et al. [29] have observed $MoO_3$ formation at 527 °C in oxygen at 400 Pa while Kim and Lieber [30], using atomic force microscopy have reported $MoO_3$ formation on single-crystal $MoS_2$ after atmospheric oxygen exposure at 480 °C for 10 min.

The occurrence of thermally induced recrystallization complicates studies of the kinetics of $MoS_2$ oxidation that use higher temperatures to accelerate reactions (and obtain activation energies). In pure oxygen, without water vapor, in the conditions studied, recrystallization occurs before or with oxidation. Of greater interest is the study of $MoS_2$ oxidation in humid air environments, which can occur at room temperature. These experiments should be conducted within time–temperature combinations that avoid recrystallization. Our experience with the UHV transmission electron microscope indicates that the instrument provides a useful pathfinder capability in kinetics experiments to find such transformation boundaries with limited samples quickly. Once known, these boundaries help to define an experimental matrix consisting of several samples at different annealing conditions. After thermal processing, these samples can be characterized by conventional TEM.

UHV TEM can clearly characterize $MoS_2$ films after in-situ heating or metal deposition, two known process-

ing variables. The apparent stability of Au evaporated onto $MoS_2$ is very surprising. These results will have to be compared with the structure of $MoS_2$ films co-sputtered with Au or having Au multilayers. One drawback to our present investigation is that the Au was deposited onto $MoS_2$ films exposed to air; the nature and role of adsorbed contaminants is unknown. Even in case of the as-deposited samples, changes in morphology are observed within the same type of films (AT or HT) and are not surprising since water vapor which influences the morphology is the major residual gas in the deposition system (base pressure, about $1 \times 10^{-4}$ Pa); these results demonstrate that it is imperative to attach an UHV sputter deposition chamber to the UHV transmission electron microscope to characterize the structure of very pure films grown under well-controlled conditions.

## 5. Conclusions

(1) The sputter-deposited $MoS_2$ films investigated are nanophase materials which undergo significant recrystallization during thermal annealing in UHV at 550 °C. Films deposited at 70 °C were less stable thermally than films deposited at 220 °C.

(2) Oxidation occurred during annealing at 550 °C in an oxygen atmosphere at $1 \times 10^{-4}$ Pa. Future studies of oxidation, particularly in humid air environments, that attempt to use elevated temperatures to accelerate reactions, will have to stay below recrystallization temperatures.

(3) UHV TEM can also be used to study film deposition issues. Au was successfully deposited onto $MoS_2$ in situ. The Au particles had unusually strong stability on basal oriented $MoS_2$ relative to Au on SiO or Au on carbon. Nucleation was seen on both basal and edge-oriented $MoS_2$.

(4) Finally, it would be desirable to characterize both the heating and the deposition characteristics of sputter-deposited $MoS_2$ films prepared under stringent UHV conditions to eliminate uncertain contamination artifacts.

## Acknowledgments

Work was sponsored by the Air Force Material Command, Space and Missile Systems Center, under Contract FO4701-93-C-0094 as part of The Aerospace Corporation Mission-Oriented Investigation and Experimentation Program and the US Air Force Office of Scientific Research on Grant F49620-93-1-0208 AFOSR. The authors wish to thank Reinhold Bauer (Aerospace Corporation) for preparing the $MoS_2$ films and R. Plass and R. Passeri (Northwestern University) for designing the heater stage and preparing the SiO grids.

## References

[1] T. Spalvins, *ASLE Trans.*, 14 (1971) 267; 17 (1973) 1; *Thin Solid Films*, 96 (1982) 17.
[2] M.R. Hilton and P.D. Fleischauer, *New Material Approaches to Tribology: Theory and Applications, Materials Research Society Symp. Proc.*, Vol. 140, Material, Research Society, Pittsburgh, PA, 1989, p. 227.
[3] M.R. Hilton and P.D. Fleischauer, *J. Mater. Res.*, 5(2) (1990) 406.
[4] P.D. Fleischauer and R. Bauer, *Tribol. Trans.*, 31(2) (1988) 239.
[5] M.R. Hilton, R. Bauer and P.D. Fleischauer, *Thin Solid Films*, 188 (1990) 216.
[6] P.D. Fleischauer and L.U. Tolentino, *Proc. 3rd Int. Conf. on Solid Lubrication*, in *Spec. Publ. ASLE SP-14*, 1984, p. 223, (Society of Tribologists and Lubrication Engineers).
[7] P.D. Fleischauer, *ASLE Trans.*, 27(1) (1983) 82.
[8] P.D. Fleischauer and T.B. Stewart, Effects of crystallite orientation on the oxidation of $MoS_2$ thin films, *Tech. Rep.*, *TR-0089A*(5945-03)-02, 9 September 1985 (The Aerospace Corporation).
[9] E.W. Roberts, *Proc. Inst. Mech. Eng. Conf. in Tribology—Friction, Lubrication, and Wear, Fifty Years On*, Vol. 1, London, Institution of Mechanical Engineers, 1987, p. 503.
[10] T.B. Stewart and P.D. Fleischauer, *Inorg. Chem.*, 21 (1982) 2426.
[11] L.E. Pope and J.K.G. Panitz, *Surf. Coat. Technol.*, 36 (1988) 341.
[12] M.R. Hilton and P.D. Fleischauer, *Surf. Coat. Technol.*, 54–55 (1992) 435.
[13] B.C. Stupp, *Thin Solid Films*, 84 (1981) 257.
[14] B.C. Stupp, *Proc. 3rd Int. Conf. on Solid Lubrication*, in *Spec. Publ. ASLE SP-14*, 1984, p. 217 (Society of Tribologists and Lubrication Engineers).
[15] M.R. Hilton, R. Bauer, S.V. Didziulis, M.T. Dugger, J. Keem and J. Scholhamer, *Surf. Coat. Technol.*, 53 (1992) 13.
[16] P. Niederhauser, H.E. Hintermann and M. Maillat, *Thin Solid Films*, 108 (1983) 209.
[17] C. Muller, C. Menoud, M. Maillat and H.E. Hintermann, *Surf. Coat. Technol.*, 36 (1988) 351.
[18] A. Aubert, J.Ph. Nabot, J. Etnoult and Ph. Renoux, *Surf. Coat. Technol.*, 41 (1990) 127.
[19] R.N. Bolster, I.L. Singer, J.C. Wegand, S. Fayeulle and C.R. Gossett, *Surf. Coat. Technol.*, 46 (1991) 207.
[20] S.D. Walck, M.S. Donley, J.S. Zabinski and V.J. Dyhouse, *J. Mater. Res.*, 9(1) (1994) 236, and earlier references cited therein.
[21] Th. Le Mogne, Y. Chevallier, Ch. Donnet and J.M. Martin, *Proc. 5th Eur. Space Mechanisms and Tribology Conf.*, in *Publ. ESA SP-334*, 1992, p. 317 (European Space Agency) ESTEC, Noordwijk.
[22] C. Donnet, Th. Le Mogne and J.M. Martin, *Surf. Coat. Technol.*, 62 (1993) 406.
[23] J.E. Bonevich and L.D. Marks, *Microsc. Key Res. Tool*, 22(1) (1992) 95.
[24] J.R. Lince, M.R. Hilton and A.S. Bommannavar, *Surf. Coat. Technol.*, 43–44 (1990) 640.
[25] J. Moser and F. Lévy, *J. Mater. Res.*, 8(1) (1993) 206, and earlier references cited therein.
[26] S.R. Singh and L.D. Marks, unpublished, 1990.
[27] N. Doraiswamy and L.D. Marks, *Z. Phys. D*, 26 (1993) S70.
[28] E.L. McMurtrey, *Lubrication Handbook for the Space Industry*, Part A: *Solid Lubricants*, In *Tech. Memo. NASA TM-86556*, 1985 (Marshall Space Flight Center, National Aeronautics and Space Administration).
[29] R.T.K. Baker, J.J. Chludzinski, Jr. and R.D. Sherwood, *J. Mater. Sci.*, 22 (1987) 3831.
[30] Y. Kim and C.M. Lieber, *Science*, 257 (1992) 297.

## TECHNOLOGY OPERATIONS

The Aerospace Corporation functions as an "architect-engineer" for national security programs, specializing in advanced military space systems. The Corporation's Technology Operations supports the effective and timely development and operation of national security systems through scientific research and the application of advanced technology. Vital to the success of the Corporation is the technical staff's wide-ranging expertise and its ability to stay abreast of new technological developments and program support issues associated with rapidly evolving space systems. Contributing capabilities are provided by these individual Technology Centers:

**Electronics Technology Center:** Microelectronics, VLSI reliability, failure analysis, solid-state device physics, compound semiconductors, radiation effects, infrared and CCD detector devices, Micro-Electro-Mechanical Systems (MEMS), and data storage and display technologies; lasers and electro-optics, solid state laser design, micro-optics, optical communications, and fiber optic sensors; atomic frequency standards, applied laser spectroscopy, laser chemistry, atmospheric propagation and beam control, LIDAR/LADAR remote sensing; solar cell and array testing and evaluation, battery electrochemistry, battery testing and evaluation.

**Mechanics and Materials Technology Center:** Evaluation and characterization of new materials: metals, alloys, ceramics, polymers and composites; development and analysis of advanced materials processing and deposition techniques; nondestructive evaluation, component failure analysis and reliability; fracture mechanics and stress corrosion; analysis and evaluation of materials at cryogenic and elevated temperatures; launch vehicle fluid mechanics, heat transfer and flight dynamics; aerothermodynamics; chemical and electric propulsion; environmental chemistry; combustion processes; spacecraft structural mechanics, space environment effects on materials, hardening and vulnerability assessment; contamination, thermal and structural control; lubrication and surface phenomena; microengineering technology and microinstrument development.

**Space and Environment Technology Center:** Magnetospheric, auroral and cosmic ray physics, wave-particle interactions, magnetospheric plasma waves; atmospheric and ionospheric physics, density and composition of the upper atmosphere, remote sensing using atmospheric radiation; solar physics, infrared astronomy, infrared signature analysis; effects of solar activity, magnetic storms and nuclear explosions on the earth's atmosphere, ionosphere and magnetosphere; effects of electromagnetic and particulate radiations on space systems; space instrumentation; propellant chemistry, chemical dynamics, environmental chemistry, trace detection; atmospheric chemical reactions, atmospheric optics, light scattering, state-specific chemical reactions and radiative signatures of missile plumes, and sensor out-of-field-of-view rejection.